Journal of Solid State Chemistry **147,** 664–670 (1999)
Article ID jssc.1999.8444, available online at http://www.idealibrary.com on IDEAL®

Insertion of Gallium Oxide into α-Titanium Phosphate Using a Surfactant Expanded Phase as Precursor

J. Jiménez-Jiménez, P. Maireles-Torres, A. Jiménez-López, and E. Rodríguez-Castellón

Departamento de Química Inorgánica, Cristalografía y Mineralogía, Facultad de Ciencias, Universidad de Málaga, 29071 Málaga, Spain

Received February 22, 1999; in revised form May 11, 1999; accepted July 2, 1999

Intercataled gallium oxide in α-titanium phosphate materials can be synthesized using a swelled phase such as cetyltrimethylammonium titanium phosphate as precursor. This is prepared in a single step by hydrolysis of titanium iso-propoxide with phosphoric acid via a supramolecular long-range ordered organic species acting as a template, which by cationic exchange with gallium oligomers and ulterior calcination at 823 K gives rise to mesoporous solids. These materials exhibit high specific surface areas close to 150 $m^2 g^{-1}$, high acidity predominantly of the Lewis type, which are active as catalysts in the conversion of the 2-propanol dehydration reaction at 493 K with conversions ranging between 50 and 83%, and total selectivities for propene. © 1999 Academic Press

Key Words: **titanium phosphate; gallium oxide; pillared materials; mesoporous solids; acid solids; acid catalysts.**

INTRODUCTION

In 1992, the synthesis of mesoporous solids underwent a remarkable change with the finding of new M41S solids by researchers at Mobil (1). In the synthesis of these new materials surfactant molecules are used as a template for the structuration of an inorganic framework. Three organo-inorganic geometries are possible to obtain: hexagonal (MCM-41), cubic (MCM-48), and lamellar. In the case of hexagonal and cubic structures, when the surfactant is removed, porous materials are obtained. This fact explains the current importance of hexagonal and cubic structures in the field of porous materials preparation. However, for lamellar phases, the removal of the template does not give rise to porous materials because collapsed structures are always obtained (2). But the preparation of highly expanded lamellar structures with surfactants is very useful as a precursor for other purposes such as starting materials which form pillared layered structures (PLS) with inorganic oxides. This new technique of synthesis consists of the intercalation of metallic oligomeric species by cationic exchange of surfactants into the interlayer region of lamellar hosts. After a mild thermal process, metal oxide nanoparticles are formed permanently holding apart the host layers and creating micro- and mesoporosity in these solids. Different layered compounds have been employed as starting substances such as clays, metal(IV) layered phosphates, and double hydroxides (3).

Pillared clay materials are used as catalysts in reactions such as gas oil cracking to yield gasoline, disproportionation processes, alkylation of toluene, etc. (4). In the case of metal(IV) layered phosphates, α-zirconium phosphate is the host matrix most commonly used, and alumina, chromia, or gallium oxide pillared phosphates have been obtained. Other members of this layered phosphate family are α-titanium phosphate and α-tin phosphate, which have been used as layered structures to obtain PLS too (3). In both cases, prior to the intercalation of polyhydroxocations, it is necessary to expand the layered structure by intercalation of organic molecules such as alkyl amines or tetraalkylammonium cations (5). Using surfactants as a template we have already obtained gallium oxide pillared α-zirconium phosphate materials by the insertion of gallium oligomer species into the host phosphate structure via an ion exchange of dodecyltrimethylammonium cations, this being the precursor to a lamellar MCM-type dodecyltrimethylammonium-zirconium phosphate (6). Recently an analogous structure of cetyltrimethylammonium-titanium phosphate has been synthesized by a sol-gel process (7). In the present work, we have now employed this organo-inorganic phase as a starting material for the preparation of gallium oxide inserted into titanium phosphates which have been fully characterized, and their acid catalytic properties have been evaluated.

EXPERIMENTAL

Synthesis of the Lamellar Phase Cetyltrimethylammonium-Titanium Phosphate

The synthesis of the lamellar cetyltrimethylammonium-titanium phosphate phase (CTMA-TiP) was carried out using the general method previously described for obtaining MCM-type materials. Thus, an orthophosphoric acid solution (85%) was added to cetyltrimethylammonium bromide

0022-4596/99 $30.00

solution in *n*-propanol. After aging this solution for 30 min at 373 K, titanium tetra-iso-propoxide dissolved in *n*-propanol was slowly added under vigorous stirring. The P/Ti molar ratio was 2, as in the case of titanium phosphate, while the CTMA/Ti molar ratio was 1.12. This was the minimum molar ratio necessary to get a saturated CTMA-TiP lamellar phase (7). The obtained gel was stirred for 3 days at 423 K under hydrothermal conditions. The white solid was removed by centrifugation and washed with *n*-propanol–water (1 : 1), later with distilled water up to pH 3, and finally air dried at 333 K.

Preparation of Gallium Oligomeric Solutions

An aqueous solution 0.7 M of $Ga(NO_3)_3$ was hydrolyzed by dropwise addition of 0.1 M *n*-propylamine aqueous solution under vigorous stirring until a base/metal molar ratio of 2.5 was obtained. The hydrolyzed solution was aged at 323 K for 30 min and quickly cooled in an ice bath. Under these experimental conditions, oligomeric Ga_{13} ions with a Keggin structure are obtained according to the literature (8).

Insertion of Oligomeric Gallium Species into Titanium Phosphate Host

The oligomeric gallium solution was added dropwise to a colloidal suspension of the CTMA-TiP in water (2 wt%) and refluxed for 3 days. The white solid phase was isolated by centrifugation, washed with distilled water, and dried at 333 K. This precursor material was calcined at 823 K for 5 h in order to obtain intercalated gallium oxide nanoparticles between the layers of the titanium phosphate host.

Several materials were obtained by addition of a different Ga/P molar ratio. These solids were labeled as Ga-TiP *x* for precursors and calc-Ga-TiP *x* for calcined materials, where *x* is the Ga/P molar ratio added.

Characterization

For chemical analysis, all materials were previously dissolved in an aqueous HF solution. Ga and Ti contents were determined by atomic absorption spectrophotometry using a Perkin–Elmer A3100 instrument, while P content was determined colorimetrically (9). Differential and thermogravimetric analyses (DTA-TG) were carried out under static air conditions using a Rigaku Thermoflex TG 8110 instrument, at 10 K min^{-1} heating rate (calcined Al_2O_3 as a reference). X-ray powder diffraction (XRD) patterns of solids were recorded on a Siemens D501 diffractometer using Cu$K\alpha$ radiation and a graphite monochromator. XPS analyses of pillared materials were carried out using a Physical Electronics 5700 instrument with Al$K\alpha$ ($h\nu = 1486.6$ eV) and Mg$K\alpha$ ($h\nu = 1253.6$ eV) as X-ray excitation sources and a multichannel hemispherical electron analyzer. The residual pressure in the analysis chamber was maintained below 10^{-9} Torr for data acquisition. The binding energies were obtained with an accuracy of ± 0.1 eV and by charge referencing with the position of the C 1*s* peak at 284.8 eV. Scanning electron microscopy (SEM) images were obtained with a JEOL SM 840 microscope. Nitrogen adsorption–desorption isotherms of calcined materials were obtained in a conventional volumetric apparatus at 77 K. The samples were previously outgassed at 473 K and 10^{-4} Torr overnight. Thermal-programmed desorption of ammonia (TPD-NH_3) was used to determine the total acidity of the calcined materials. Before ammonia absorption at 373 K, the samples were heated at 823 K in a He flow. The TPD-NH_3 was carried out between 373 and 840 K, at 10 K min^{-1}, and analyzed by an on-line Shimadzu GC-14A gas chromatograph with a thermal conductivity detector. The nature of the acid sites of calcined materials was determined by IR analysis (Perkin–Elmer 883 infrared spectrophotometer) of adsorbed pyridine on self-supported wafers. The samples were placed in a vacuum cell provided with greaseless stopcocks and CaF_2 windows and were evacuated at 623 K and 10^{-4} Torr overnight before their exposition to pyridine vapor and outgassed at room temperature, 373, 493, and 623 K. Acid catalytic properties of calcined materials were tested in the conversion reaction of 2-propanol at 493 K in a fixed bed of tubular glass working at atmospheric pressure and using about 30 mg of catalyst without dilution. The 2-propanol was fed into the reactor by bubbling a flow of He of 25 cm^3 min^{-1} through a saturator-condenser at 303 K, which allowed a constant 2-propanol flow of 7.5 vol% and a spatial velocity of 46 μmol s^{-1} g^{-1}. Before the catalytic test, the samples were pretreated at 593 K in a He flow for 3 h. The reaction products were analyzed with an on-line gas chromatograph Shimadzu GC-14A with a flame ionization detector and a fused silica capillary column SPB1.

RESULTS AND DISCUSSION

The efficiency of the cationic exchange of CTMA organic cations by gallium oligomer species can be deduced comparing the chemical compositions of the intercalates prepared with different Ga/P molar ratios with that of the precursor exchanger which are compiled in Table 1. The presence of ionic surfactant CTMA in the Ga-TiP precursor solids, verified by DTA-TG (Fig. 1) and IR, implies the need of a high calcination temperature (823 K) for gallium oxide pillar formation and total surfactant removal (10).

The evolution of the Ga/P molar ratio taken up by the phosphate for calcined materials points to the formation of a gallium saturated solid when the Ga/P molar ratio added is 1.8 (Fig. 2). In these conditions, the Ga/P molar ratio in the solid is close to 1.3. This value is similar to that found for

TABLE 1
Chemical Compositions and Empirical Formulae for Ga-TiP Precursors and calc-Ga-TiP Materials

Sample	% H_2O	% CTMA	% Ga	Empirical formulae
CTMA-TiP	3.5	33.1	—	$TiCTMA_{0.44}H_{1.56}(PO_4)_2 \cdot 0.8H_2O$
Ga-TiP 0.5	10.0	13.2	11.6	$Ti(Ga_{13})_{0.06}CTMA_{0.20}H_{1.40}(PO_4)_2 \cdot 2.5\ H_2O$
Ga-TiP 0.9	10.0	14.6	18.7	$Ti(Ga_{13})_{0.14}CTMA_{0.28}H_{0.84}(PO_4)_2 \cdot 3.3\ H_2O$
Ga-TiP 1.8	18.0	4.6	26.2	$Ti(Ga_{13})_{0.18}CTMA_{0.13}H_{0.64}(PO_4)_2 \cdot 6.2\ H_2O$
Ga-TiP 3.7	22.5	3.7	24.7	$Ti(Ga_{13})_{0.17}CTMA_{0.10}H_{0.62}(PO_4)_2 \cdot 6.8\ H_2O$
calc-Ga-TiP 0.5	6.0	—	16.6	$Ti(Ga_2O_3)_{0.37}(HPO_4)_2 \cdot 1.0\ H_2O$
calc-Ga-TiP 0.9	7.2	—	27.8	$Ti(Ga_2O_3)_{0.96}(HPO_4)_2 \cdot 2.0\ H_2O$
calc-Ga-TiP 1.8	6.8	—	34.6	$Ti(Ga_2O_3)_{1.13}(HPO_4)_2 \cdot 1.7\ H_2O$
calc-Ga-TiP 3.7	7.0	—	32.8	$Ti(Ga_2O_3)_{1.10}(HPO_4)_2 \cdot 1.5\ H_2O$

gallium oxide inserted into zirconium phosphate (6). Therefore, the Ga-TiP system has a similar behavior to the analogous Ga-ZrP materials. On the other hand, the P/Ti molar ratio found was close to 2 in all the calc-Ga-TiP materials; a characteristic value for α-titanium phosphate.

The evidence to prove the intercalation of gallium polyhydroxocation species into titanium phosphate can be obtained from the differences observed between the XRD patterns of the CTMA-TiP starting material and the Ga-TiP precursors (Fig. 3). For the CTMA-TiP material a main reflection at 29.7 Å is observed. This d_{001} reflection corresponds to titanium phosphate intercalated by CTMA cations, with the long alkyl chain largely imbricated. The high stability of this intercalate, which presents a very high degree of compactness, requires severe conditions for the cationic exchange of this surfactant by the gallium polyhydroxo species (three days and reflux). Under these conditions, the formation of a single type of gallium oligomeric species such as Keggin cations is not possible, owing to the critical conditions necessary for that purpose (8), and so several species with different sizes are formed. As a consequence of this fact the Ga-TiP precursors become amorphous solids (Fig. 3b). Therefore, the absence of the reflection at 29.7 Å in the precursor Ga-TiP indicates the evolution from an organic structure intercalated between the layers of titanium phosphate host to another inorganic structure with a different array and low crystallinity. After calcination of this precursor material at 823 K, the XRD patterns indicate the existence of another amorphous solid, owing to the presence of gallium oxide nanoparticles with different sizes between the host layers of a very disordered solid (Fig. 3c).

Interestingly the typical reflections corresponding to GaOOH and Ga_2O_3 are not present either in the Ga-TiP precursors or in the calc-Ga-TiP materials. The absence of these peaks reveals that those species are only present as nanoparticles in the interlayer region (pillars) and not coprecipitated. In contrast, when a single oligomeric solution of gallium is treated under the same experimental conditions as those used in the intercalation process to obtain Ga-TiP

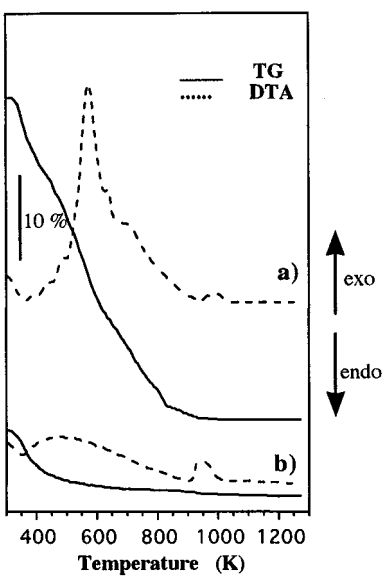

FIG. 1. TG-DTA curves of (a) Ga-TiP 0.9 precursor and (b) calc-Ga-TiP 0.9.

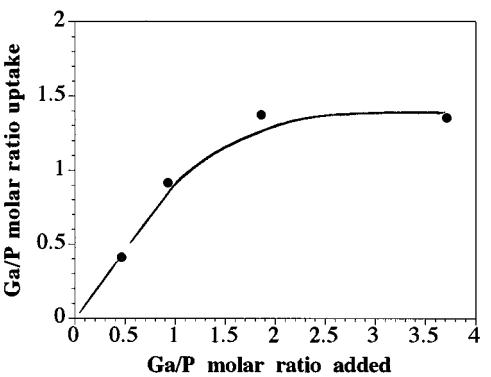

FIG. 2. Ga/P molar ratio uptake in calc-Ga-TiP solids versus Ga/P molar ratio added to the colloidal suspension of CTMA-TiP.

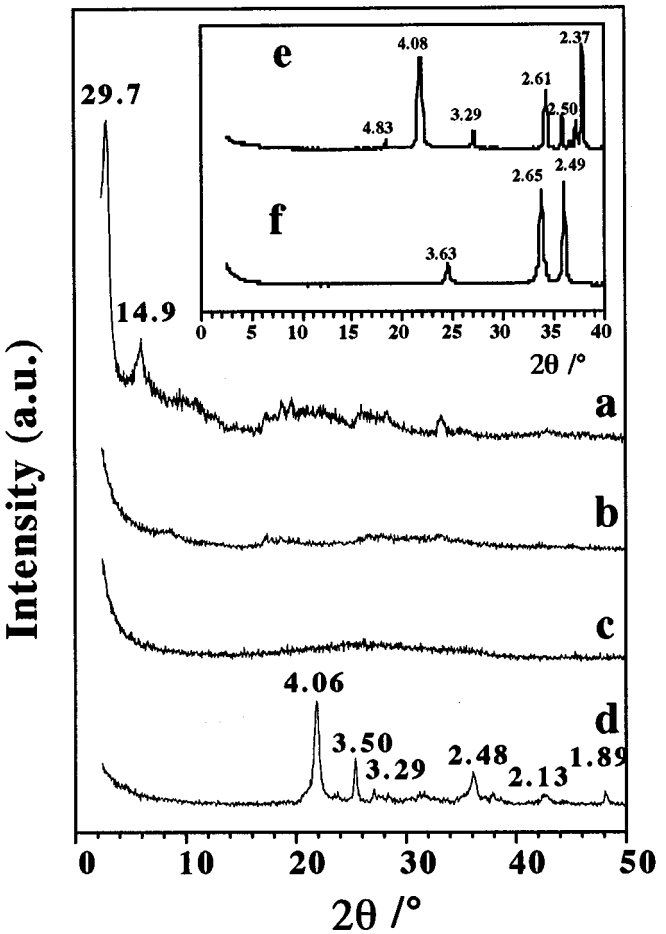

FIG. 3. XRD patterns of (a) CTMA-TiP starting material, (b) Ga-TiP 0.9 precursor, (c) calc-Ga-TiP 0.9, (d) calc-Ga-TiP 0.9 at 1273 K, (e) GaOOH precipitated from a gallium oligomeric solution, and (f) α-Ga_2O_3.

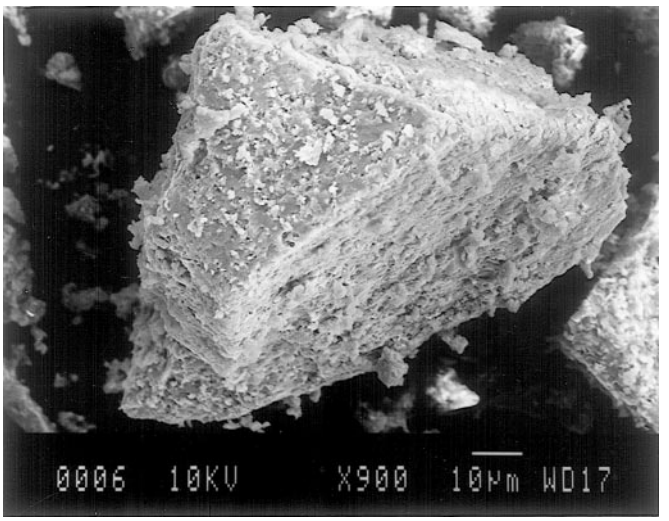

FIG. 4. SEM micrographs of Ga-TiP 0.9 material.

precursors, a white and highly crystalline solid is formed, whose XRD patterns exhibit the characteristic reflections of GaOOH. This solid at 673 K originates α-Ga_2O_3 (Fig. 3f). This behavior is very different from that observed for Ga-TiP precursors, which appear to be amorphous even after calcination at 873 K. Only after calcination at 1273 K, the XRD patterns show several reflections at 4.06, 3.50, 2.48, and 2.13 Å, corresponding to gallium phosphate, together with another set of peaks at 3.50, 2.37, and 1.89 Å assigned to TiO_2. The absence of titanium pyrophosphate after this thermal treatment demonstrates once more that the gallium oxide was intercalated between the layers of α-TiP, avoiding the formation of pyrophosphate upon calcination. The lamellar structure of these calc-Ga-TiP materials can be observed in the SEM micrograph images of Fig. 4. Thus, after the cationic exchange and calcination processes, the lamellar structure of the titanium phosphate host matrix is preserved.

Surface Properties of Calcined Ga-Tip Materials

XPS is a very useful technique to study the surface composition of solids. The Ga/P superficial molar ratios of calc-Ga-TiP obtained by this technique are similar to the Ga/P bulk values found by chemical analysis. This analogy is closer for the samples with a lower Ga/P molar ratio added, although a little divergence appears for the sample with the higher Ga/P molar ratio (Fig. 5). However, these data let us consider these materials as homogeneous phases.

The binding energy (BE) values of Ga 2*p* in the calcined solids appear at 1118.4 eV which are higher than that corresponding to pure gallium oxide (1117.3 eV). This difference can originate as a consequence of the strong interaction between the nanoparticles of gallium oxide guest with the

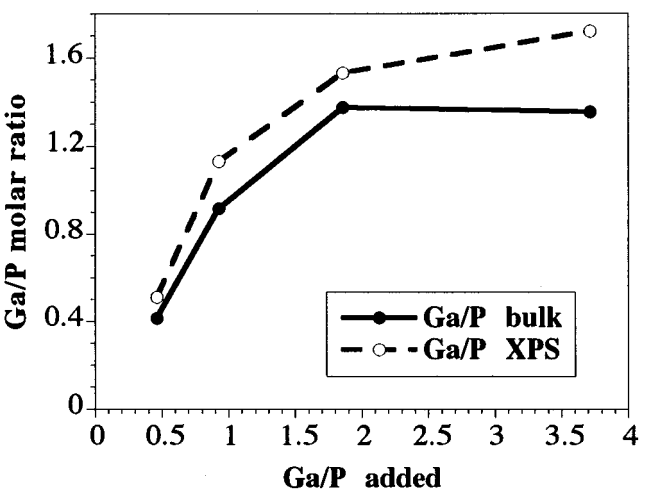

FIG. 5. Bulk and surface (XPS) Ga/P ratios in calc-Ga-TiP materials corresponding to the different Ga/P molar ratio added.

layers of the titanium phosphate host. Even so, these values also preclude any coprecipitattion of Ga_2O_3.

Textural parameters of calcined Ga-TiP materials are obtained by analysis of adsorption–desorption N_2 isotherms at 77 K. In all cases the isotherms are type IV of IUPAC classification (11), typical of mesoporous solids (Fig. 6), although the initial adsorption at low relative pressures is indicative of the existence of some micropores. Structurally, the micropores are assigned to the voids located between gallium oxide particles within the phosphate interlayer region, while mesopores are created principally by edge–edge and edge–face interactions between the different platelets. The textural parameter values are summarized in Table 2. High values of S_{BET} have been obtained, especially in comparison with pure α-titanium phosphate ($< 10\ m^2\ g^{-1}$), CTMA-TiP starting phase calcined at 823 K ($40\ m^2\ g^{-1}$), or gallium oxide ($51\ m^2\ g^{-1}$). Therefore the S_{BET} values of the calc-Ga-TiP solids are a consequence of the presence of gallium oxide particles between the titanium phosphate layers. However, there are not noticeable differences for S_{BET} of these solids. Thus, the calc-Ga-TiP 0.9 has the highest specific surface area ($146\ m^2\ g^{-1}$), while the samples with the maximum gallium content have similar S_{BET} values, being close to $120\ m^2\ g^{-1}$. The pore size distribution (insert in Fig. 6), obtained by using the Cranston and Inkley method (12), indicates the presence of mesopores in a large interval of radii and with two maxima at 20 and 45 Å.

The acid properties of calcined materials have been studied by three different techniques, TPD-NH_3, IR study of adsorbed pyridine, and the catalytic test of the 2-propanol reaction. The total acidity of calc-Ga-TiP materials was obtained by use of TPD-NH_3. Ammonia can neutralize both Brønsted and Lewis acid centers. The TPD-NH_3 curves do not show a defined maximum, clearly indicating that a broad distribution of acid sites with different strengths is present in these solids. The total acidity values, obtained by integration of the area under the TPD-NH_3 curves, are shown in Fig. 7. These values are comparable with those corresponding to other pillars prepared in metal(IV) phosphate (13) or clays (14). The total acidity decreases with the Ga/P molar ratio loading, from

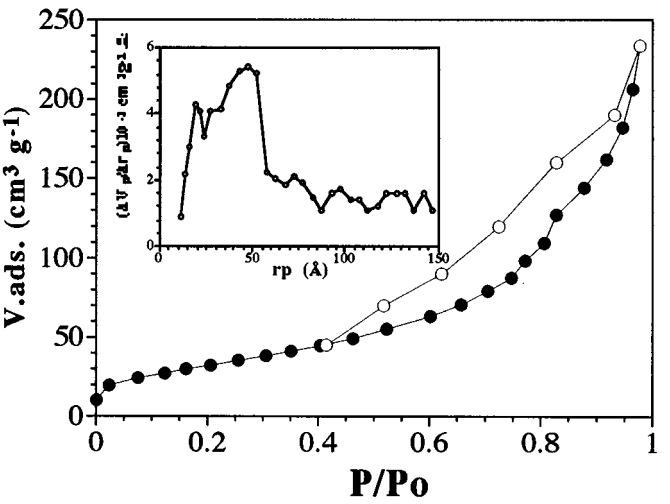

FIG. 6. Adsorption–desorption isotherms of N_2 at 77 K and pore size distribution (insert) of calc-Ga-TiP 0.9 material.

934 μmol g^{-1}, for the calc-Ga-TiP 0.5 sample to 239 μmol g^{-1} for the calc-Ga-TiP 3.7 sample. This behavior was also observed in other similar systems (15) and can be explained by the progressive decrease in the number of accessible Brønsted acid sites associated with P-OH groups, provoked by increasing gallium oxide insertion and by the production of stuffed structures in which the accessibility to the acid sites becomes more difficult. It can be seen in Fig. 7 that in all cases, a higher percentage of acid sites are desorbed between 573 and 773 K. This fact reveals the existence of strong acid sites in these materials.

By using IR studies of adsorbed pyridine on the samples and ulterior desorption at different temperatures, the percentage of Brønsted and Lewis acid sites can be evaluated

TABLE 2
Textural Parameters of calc-Ga-TiP Materials

Sample	S_{BET} (m^2g^{-1})	C_{BET}	S_{ac} [a] (m^2g^{-1})	$\sum Vp$ [a] (cm^3g^{-1})	dp(av) [a] (Å)	V_{micro} [b] (cm^3g^{-1})
calc-Ga-TiP 0.5	134	90	198	0.337	82	0.049
calc-Ga-TiP 0.9	146	58	245	0.521	78	0.054
calc-Ga-TiP 1.8	120	82	159	0.317	87	0.046
calc-Ga-TiP 3.7	124	80	170	0.342	84	0.047

[a] From Cranston–Inkley method.
[b] From Dubinin–Radushkevich equation (12).

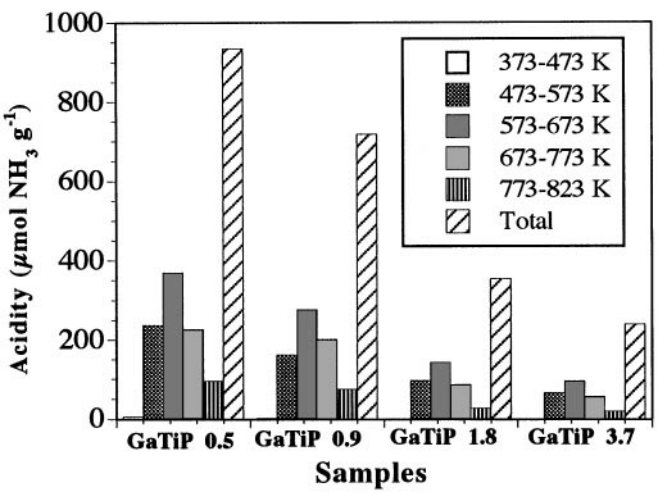

FIG. 7. Total acidity of calc-Ga-TiP materials obtained by TPD-NH_3 analysis.

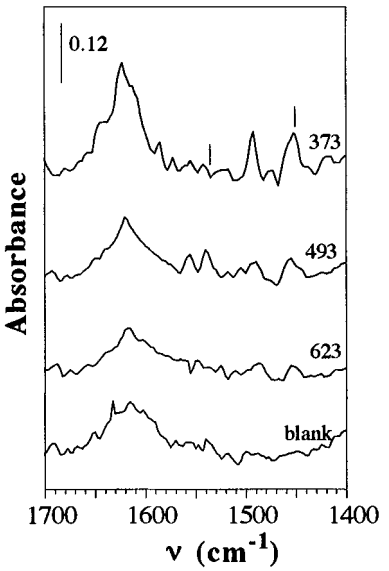

FIG. 8. IR spectra of calc-Ga-TiP 0.9 exposed to pyridine and outgassed at 493 and 623 K.

(16). The band at 1550 cm^{-1} is assigned to the pyridinium ion formed on a Brønsted acid site, while the band at 1450 cm^{-1} corresponds to pyridine coordinated to a Lewis site (Fig. 8). Structurally, the Brønsted acid sites are associated with P-OH on the surface of the layers of titanium phosphate and GaOH groups of pillars, while the Lewis acid sites are associated with gallium cations with unsaturated coordination in the pillars of gallium oxide. On the other hand, as gallium oxide is located as nanoparticles between the layers of titanium phosphate, there is a direct relationship between the Ga/P molar ratio of the calc-Ga-TiP solids and their concentration of Lewis acid sites at 373 K, as is clearly observed in Fig. 9. However, the concentration of Brønsted acid sites is very low and has not been considered.

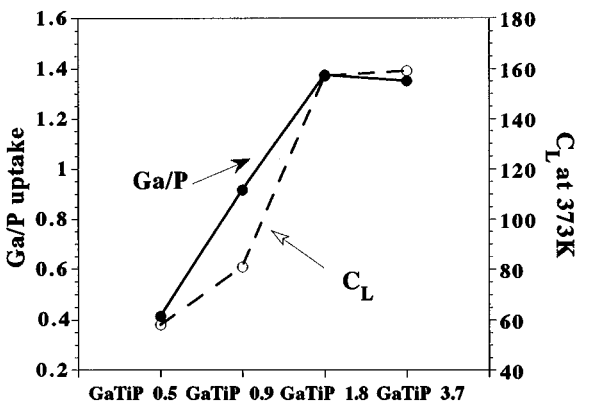

FIG. 9. Concentration of Lewis acid sites versus the Ga/P molar ratio uptake for the different calc-Ga-TiP materials.

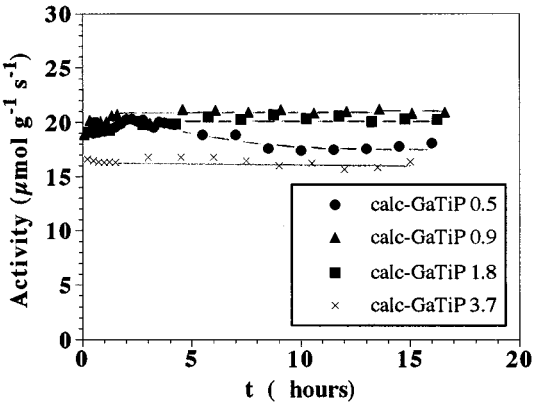

FIG. 10. Catalytic activity of calc-Ga-TiP materials for the conversion of 2-propanol as a function of time on stream at 493 K.

The efficiency of these new materials as acid solid catalysts is tested in the 2-propanol conversion reaction. This reaction test determines the presence of acid and/or redox centers on the surface of solids, through the evaluation of the possible products of reaction: propene or acetone. As expected for the calc-Ga-TiP materials only propene is obtained (dehydrating product). For all samples, the activation energy was determined for this reaction in the temperature interval of 423 and 573 K. The experimental values ranged between 28.7 and 31.7 kcal mol^{-1}; therefore, the catalytic reaction was not controlled by the diffusion of 2-propanol molecules (17). The evolution of activity with time on stream for the different samples is shown in Fig. 10. The activities of these materials are in the range of 16–21 μmol g^{-1} s^{-1}, not exhibiting any deactivation after 16 h of reaction. When the catalytic activity of these catalysts and their total acidity obtained by TPD-NH_3 is compared no direct relationship is observed. Thus the sample calc-Ga-TiP 3.7 shows a lower activity, owing to its low acidity. On the other hand, the calc-Ga-TiP 0.9 sample exhibits the highest activity in spite of their average value of total acidity. The explanation of this behavior can be given taking into account that the catalytic activity is a result of several factors such as total acidity, specific surface area, pore accessibility, number, and strength of acid sites (17). However, the activity values for calc-Ga-TiP materials are quite similar to others found in analogous systems based on Ga/Cr mixed oxides pillared α-zirconium phosphate (13) and Ga/Al oxide pillared α-tin phosphate (18), although they are lower than those obtained for gallium oxide inserted into α-zirconium phosphate materials, due to the high acidities and surface areas of the latter materials (6).

CONCLUSIONS

Cetyltrimethylammonium-expanded titanium phosphate intercalate, obtained by direct synthesis with

supramolecular long-range ordered organic species as a template, was used as starting exchanger material to prepare intercalated gallium oligomers into α-titanium phosphate host. After calcination at 823 K of the precursor materials, porous solids were obtained with acid properties and a remarkably high percentage of Lewis acid sites. The efficiency of these materials as acid catalysts was tested with the conversion of 2-propanol reaction at 493 K. In all cases 100% selectivity to propene and high conversions ranging between 50 and 83% were obtained.

ACKNOWLEDGMENTS

This research was supported by the CICYT (Spain) Project MAT 97-906. J.J.J. thanks the M.E.C. of Spain for a fellowship.

REFERENCES

1. (a) C. T. Kresge, M. E. Leonowicz, W. J. Roth, J. C. Vartulli, and J. S. Beck, *Nature* **359,** 710 (1992). (b) J. S. Beck, J. C. Vartulli, W. J. Roth, M. E. Leonowicz, C. T. Kresge, K. D. Schmitt, C. T. W. Chu, D. H. Olson, E. W. Sheppard, S. B. McCullen, J. B. Higgins, and J. L. Schlenker, *J. Am. Chem. Soc.* **114,** 10834 (1992).
2. Q. Huo, D. I. Margolese, U. Ciesla, D. G. Demuth, P. Feng, T. E. Gier, P. Sieger, A. Firouzi, B. F. Chmelka, F. Schüth, G. D. Stucky, *Chem. Mater.* **6,** 1176 (1994).
3. (a) T. J. Pinnavaia, *Science* **220,** 365 (1983). (b) F. Figueras *Catal. Rev.-Sci. Eng.* **30,** 457 (1988). (c) I. V. Mitchell, "Pillared Layered Structures: Current Trends and Applications." Elsevier Applied Science, London, 1990. (d) A. Clearfield, *in* "Multifunctional Mesoporous Inorganics Solids" (C. A. C. Sequeira and M. J. Hudson, Eds.), p. 159. NATO ASI, Kluwer Academic, Dordrecht, 1993. (e) P. Olivera-Pastor, A. Jiménez-López, P. Maireles-Torres, E. Rodriguez-Castellón, A. A. G. Tomlinson, and L. Alagna, *J. Chem Soc., Chem Commun.* **751 (**1989). (f) J. Rozière, D. J. Jones, and T. J. Cassagneau, *J. Mater. Chem.* **1,** 1081 (1991).
4. R. Burch, Ed., *Catal. Today* **2,** 1–185 (1988).
5. A. Clearfield and B. D. Roberts, *Inorg. Chem.* **27,** 3237 (1988).
6. J. Jimenez-Jimenez, P. Maireles-Torres, P. Olivera Pastor, E. Rodriguez-Castellon, and A. Jimenez-Lopez, *Langmuir* **13,** 2857 (1997).
7. J. Jimenez-Jimenez, P. Maireles-Torres, P. Olivera Pastor, E. Rodriguez-Castellon, and A. Jimenez-Lopez, *Mol. Cryst. Liq. Cryst.* **311,** 257 (1998).
8. (a) S. M. Bradley, R. A. Kydd, and R. J. Yamdagni, *J. Chem. Soc., Dalton Trans.* 413 (1990). (b) S. M. Bradley, R. A. Kydd, and R. J. Yamdagni, *J. Chem. Soc., Dalton Trans.* 2653 (1990). (c) S. M. Bradley, R. A. Kydd, and R. J. Yamdagni, *Magn. Reson. Chem.* **28,** 746 (1990). (d) S. M. Bradley, R. A. Kydd, and C. A. Fyfe, *Inorg. Chem.* **31,** 1181 (1992).
9. G. Charlot, "Chimie Analytique Quantitative," Vol. 2, 6th ed. Masson, Paris, 1974.
10. S. Hitz and R. Prins, *J. Catal.* **168,** 194 (1997).
11. K. S. W. Sing, D. H. Everett, R. A. W. Haul, L. Moscou, R. A. Pierotti, J. Rouquerol, and T. Siemieniewska, *Pure Appl. Chem.* **57,** 603 (1985).
12. R. W. Cranston and F. A. Inkley, *Adv. Catal.* **9,** 143 (1957).
13. M. Alcántara-Rodríguez, P. Olivera-Pastor, E. Rodríguez-Castellón, A. Jiménez-López, M. Lenarda, L. Storaro, and R. Ganzerla, *J. Mater. Chem.* **8,** 1625 (1998).
14. X. Tang, W.-Q. Xu, Y.-F Shen, and S. L. Suib, *Chem. Mater.* **7,** 102 (1995).
15. (a) J. M. Mérida-Robles, P. Olivera-Pastor, A. Jiménez-López, and E. Rodríguez-Castellón, *J. Phys. Chem.* **100,** 14746 (1996). (b) T. Cassagneau, G. Hix, D. Jones, P. Maireles-Torres, M. Rhomari, and J. Rozière, *J. Mater. Chem.* **4,** 189 (1994).
16. J. Datka, A. M. Turek, J. M. Jehng, and I. E. Wachs, *J. Catal.* **135,** 186 (1992).
17. G. C. Bond, "Heterogeneous Catalysis. Principles and Applications," 2nd ed. Clarendon Press, Oxford, 1987.
18. P. Braos-García, E. Rodríguez-Castellón, P. Maireles-Torres, P. Olivera-Pastor, and A. Jiménez-López, *J. Phys. Chem. B* **102,** 1672 (1998).